

ESR, electrochemical and cyclodextrin-inclusion studies of triazolopyridyl pyridyl ketones and dipyridyl ketones derivatives

C. Olea-Azar^{a,*}, B. Abarca^b, E. Norambuena^c, L. Opazo^a, C. Jullian^d,
S. Valencia^a, R. Ballesteros^b, M. Chadlaoui^b

^a *Departamento de Química Inorgánica y Analítica, Facultad de Ciencias Químicas y Farmacéuticas, Universidad de Chile, Chile*

^b *Departamento de Química Orgánica, Facultad de Farmacia, Universidad de Valencia, Spain*

^c *Departamento de Química, Universidad Metropolitana de Ciencias de la Educación, Chile*

^d *Departamento de Química Orgánica y Fisicoquímica, Facultad de Ciencias Químicas y Farmacéuticas, Universidad de Chile, Casilla 233, Santiago 1, Chile*

Abstract

The electron spin resonance (ESR) spectra of free radicals obtained by electrolytic reduction of triazolopyridyl pyridyl ketones and dipyridyl ketones derivatives were measured in dimethylsulfoxide (DMSO). The hyperfine patterns indicate that the spin density delocalization is dependent of the rings presented in the molecule. The electrochemistry of these compounds was characterized using cyclic voltammetry, in DMSO as solvent. When one carbonyl is present in the molecule one step in the reduction mechanism was observed while two carbonyl are present two steps were detected. The first wave was assigned to the generation of the correspondent free radical species, and the second wave was assigned to the dianion derivatives. The phase-solubility measurements indicated an interaction between molecules selected and cyclodextrins in water. These inclusion complexes are 1:1 with β CD, and HP- β CD. The values of K_s showed a different kind of complexes depending on which rings are included. AM1 and DFT calculations were performed to obtain the optimized geometries, theoretical hyperfine constants, and spin distributions, respectively. The theoretical results are in complete agreement with the experimental ones.

Keywords: Triazolopyridyl pyridyl ketones; Dipyridyl ketones derivatives; ESR; Cyclic voltammetry; Cyclodextrin

1. Introduction

In general, chemical or electrochemical reduction of ketones yields alcohols [1]. More specifically, in aprotic media electrochemical reductions give primarily dianions through radical-radical, radical-ketone or ion-ketone coupling [2]. Pyridine-based aromatic ketones have the same electrochemistry behaviour. Di-pyridyl ketone [(py)₂CO] have been used as ligand which have three potential donor groups, the two pyridyl nitrogens and the central oxygen [3–5]. However, the chemical characteristic of the (py)₂CO that make this ligand special; this is its carbonyl group. Ketones (R₂CO) can undergo hydration, with the first step of the reaction involving of nucle-

ofilic attack of water on the carbonyl group [6]. The tetrahedral intermediate is trapped by reaction with a proton to yield the hydrated form of the ketone, the geminal diol. Perlepes et al. have developed several work developing complexes with (py)₂CO as ligand. The structural diversity of these complexes stems from the ability of the singly and doubly deprotonated anions of the gem diol form of the (py)₂CO and its derivatives to exhibit a variety of coordination modes [7–9]. On the other hand, some related compounds of (py)₂CO as 4-acyl- and 4-benzoylpyridinium cations are reduced, generating stable radical species, which are characterized by electron spin resonance (ESR) spectroscopy [10,11]. These kinds of compounds could be considered for applications as redox mediator or electrochromic compounds [12–14]. Boudalis et al., isolated and characterized the first icosanuclear Co(II) cluster using 2,6-bis(2-pyridylcarbonyl)pyridine as ligand. The results indicated that the coordinative flexibility and versatility of this

* Corresponding author. Tel.: +56 2 9782834; fax: +56 2 7370567.
E-mail address: colea@uchile.cl (C. Olea-Azar).

ligand was useful in polynuclear metal chemistry [15]. Also, we have analyzed the electrochemical mechanism of (py)₂CO and other 2-acylpyridines and 6,6'-diacyl-2,2'-bipyridines and we have compared the reduction mechanism with that of 4-acyl- and 4-benzoylpyridinium cations family [16]. The results suggested that (py)₂CO and its derivatives compounds could be considered for applications as redox mediators or electrochromic compounds [16]. Recently, cyclodextrins have been utilized as attractive biomimetic modeling of the chemical reactions to investigate the oxidation of variety of ketone derivatives in water [17,18]. In the present work, we analyzed the electrochemistry mechanism of triazolopyridyl pyridyl ketones **1–5** and dicarbonyl derivatives **6–10** (Fig. 1). We report electrochemical and ESR studies of these families in dimethylsulfoxide (DMSO). Also, was selected to study the complexation of ketones **4**, **6**, **7** and **11** by using two different cyclodextrins (HP-βCD and βCD) to evaluate the inclusion process and improve the solubility in water. AM1 and DFT calculations were performed to obtain the optimized geometries, theoretical hyperfine constants, and spin distributions, respectively.

2. Experimental

2.1. Samples

Compounds **1**, **2**, **3**, **4**, **5** and **10**, are synthesized as described in Ref. [19], molecules **6–9** are synthesized as described in Ref. [20], molecule **11** are synthesized as described in Ref. [21].

2.2. Reagents

Dimethylsulfoxide (spectroscopy grade) and tetrabutylammonium perchlorate (TBAP), used as supporting electrolyte,

were supplied from Fluka. βCD and HP-βCD [MS (average molar degree of substitution)=1.0] were purchased from Sigma–Aldrich, Inc., St. Louis, MO.

2.3. Cyclic voltammetry

Cyclic voltammetry was carried out using a Weenking POS 88 instrument with a Kipp Zenen BD93 recorder, in DMSO (ca. 1.0×10^{-3} mol dm⁻³), under a nitrogen atmosphere, with TBAP (ca. 0.1 mol dm⁻³), using three-electrode cells. A hanging drop mercury electrode (HDME) was used as the working electrode, a platinum wire as the auxiliary electrode, and saturated calomel (SCE) as the reference electrode.

2.4. ESR spectroscopy

ESR spectra were recorded in the Xband (9.85 GHz) using a Bruker ECS 106 spectrometer with a rectangular cavity and 50 kHz field modulation. The hyperfine splitting constants were estimated to be accurate within 0.05 G. ESR spectra of the anion radical derivatives were obtained in the electrolysis solution. The ESR spectra were simulated using the program WINEPR Simphonia 1.25 Version.

2.5. Phase–solubility measurements

Phase–solubility measurements were carried out according to the method of Higuchi and Connors [22]. Excess amount of compound (4 mg) was added to 5 mL of deionized water containing increasing amounts of βCD, and HP-βCD (ranging from 0 to 0.010 M). The resulting mixture was equilibrated in a Julabo thermostatic shaking water bath for 24 h at 30 °C after which the equilibrium was reached. Then, suspensions

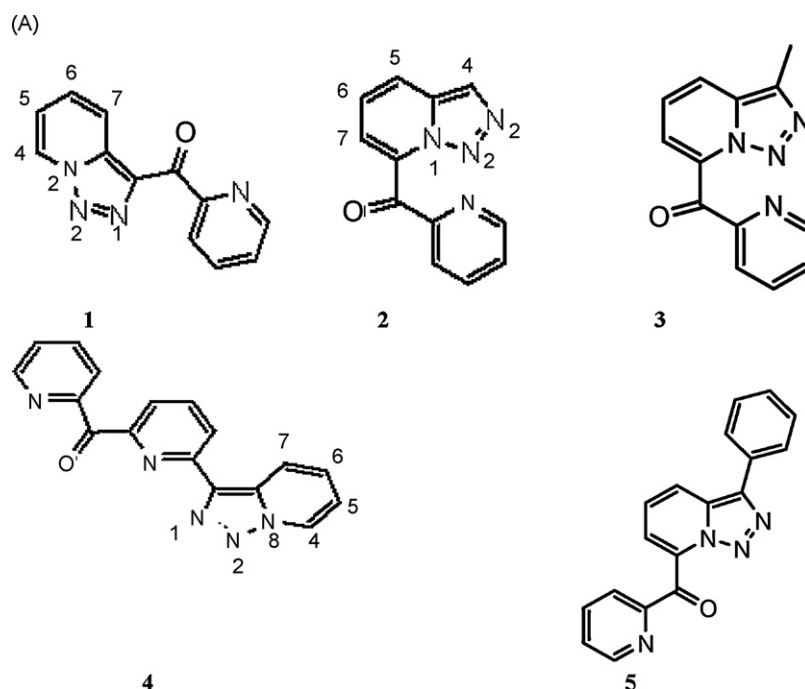


Fig. 1. (A) Triazolopyridyl pyridyl ketones and (B) dicarbonyl derivatives.

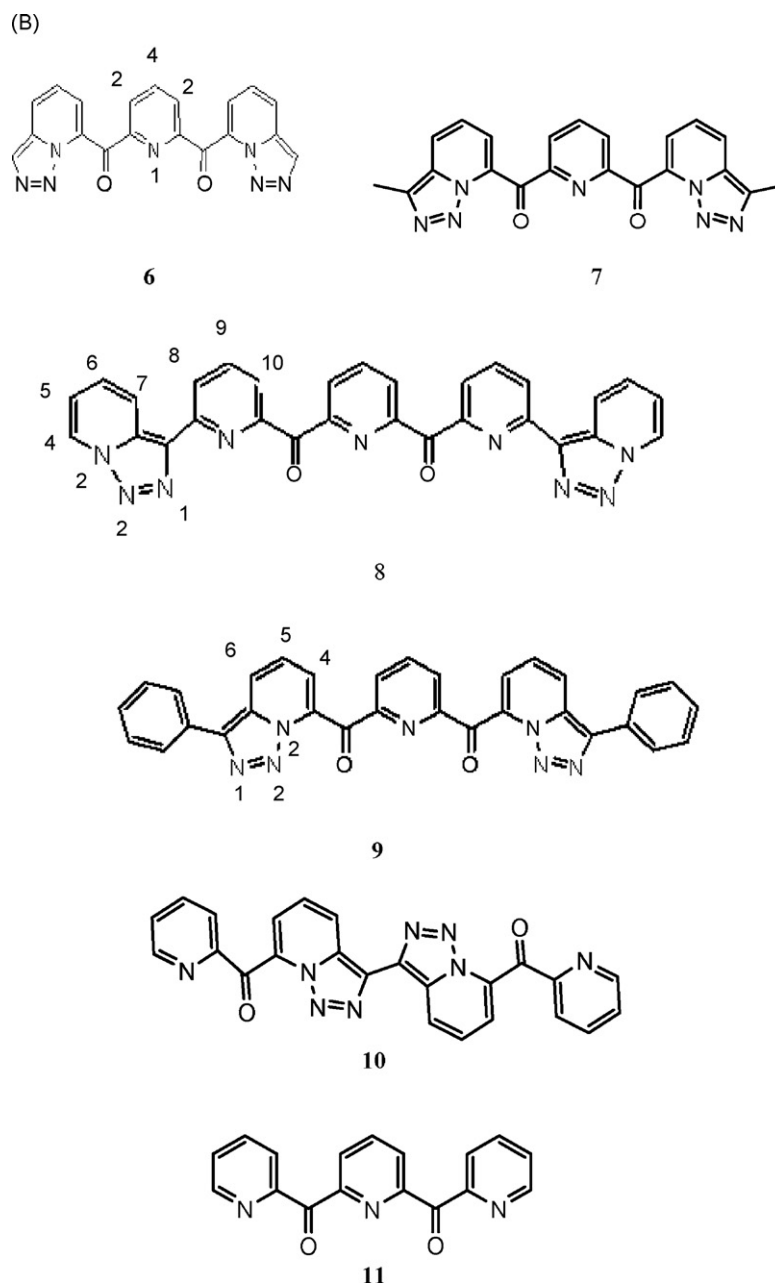


Fig. 1. (Continued).

were filtered through 0.45 μm cellulose acetate membrane filter to remove undissolved solid. An aliquot from each vial was adequately diluted and spectrophotometrically analyzed at each maximum.

The apparent stability constant (K_s) of the complexes were calculated from the phase-solubility diagrams according to the following equation:

$$K_s = \frac{\text{slope}}{S_0(1 - \text{slope})} \quad (1)$$

where S_0 is the solubility of the substrate at 30 $^\circ\text{C}$ in absence of cyclodextrin and slope means the corresponding

slope of the phase-solubility diagrams, i.e., the slope of the drug molar concentration versus CDs molar concentration graph.

Spectrophotometric measurements were carried out with a UV2 UNICAM spectrophotometer, using a 1 cm quartz cell.

2.6. Theoretical calculations

Full geometry optimizations of the compounds in spin paired and free radical forms were carried out by AM1 methodology. The theoretical hyperfine constants were obtained using B3LYP 6-31G* level.

Table 1

Cyclic voltammetric parameters of studied compounds in DMSO vs. calomel electrode

Compound	E_{pc1} (V)	E_{pa1} (V)	ΔE (V)	I_{pa1}/I_{pc1}	E_{pc2} (V)
1	-1.50	-1.42	0.08	0.8	-
2	-1.26	-1.16	0.09	0.7	-
3	-1.28	-1.19	0.09	0.7	-
4	-1.24	-1.18	0.06	0.7	-
5	-1.26	-1.18	0.08	0.9	-
6	-1.25	-1.15	0.10	0.8	-1.79
7	-1.20	-1.07	0.13	0.6	-1.54
8	-1.33	-1.23	0.10	0.7	-1.60
9	-1.14	-1.04	0.07	0.5	-1.45
10	-0.87	-0.85	0.02	0.8	-1.29

3. Results and discussion

3.1. Cyclic voltammetry

Table 1 lists the values of voltammetric peaks and the anodic and cathodic currents for all compounds. All one carbonyl-derivates, **1–5**, display comparable voltammetric behaviour, showing one well-defined reduction wave in DMSO.

This wave corresponds to a quasi-reversible one-electron transfer in DMSO. The reverse scan showed the anodic counterpart of the reduction waves. The breadth of cathodic wave at its half intensity has a relatively constant value close to 60 mV. The intensity ratio I_{pa}/I_{pc} has a value close to one. According to the standard reversibility criteria this couple corresponds to quasi-reversible diffusion controlled. Fig. 2A shows the voltamogram of compound **1** of the one-electron transfer mechanism [23].

However, the dicarbonyl derivatives show one well-defined reduction wave. The first wave corresponds to a quasi-reversible process. This couple was attributable to the reduction of a ketone to a stable anion radical at room temperature. The second cathodic peak is irreversible in the whole range of sweep rates used (50–2000 mV s^{-1}). We can attribute this wave to the production of the corresponding anion derivative. Fig. 2B shows the voltamogram of compound **7**.

Also we studied the effect of the inclusion of the compounds **4, 6, 7** and **11** in β CD by cyclic voltammetry technique. The addition of β CD to a solution of these molecules causes two changes in the first wave. Firstly, the cathodic peak potential (E_{pc}) shifted in a negative direction and secondly, the I_{pc} decreased (data not shown). These results can be ascribed to the formation of the inclusion in all case.

3.2. ESR

The electrochemical reductions (in situ) to the radical forms in DMSO were carried out applying the potential corresponding to the first wave from the cyclic voltammetry experiments for each compound. The interpretation of the ESR spectra by means of a simulation process led to the determination of the experimental coupling constants for the observed magnetic nuclei.

The hyperfine constants are listed in Table 2. Compound **1** (Fig. 3) was analyzed and simulated in term of one doublet

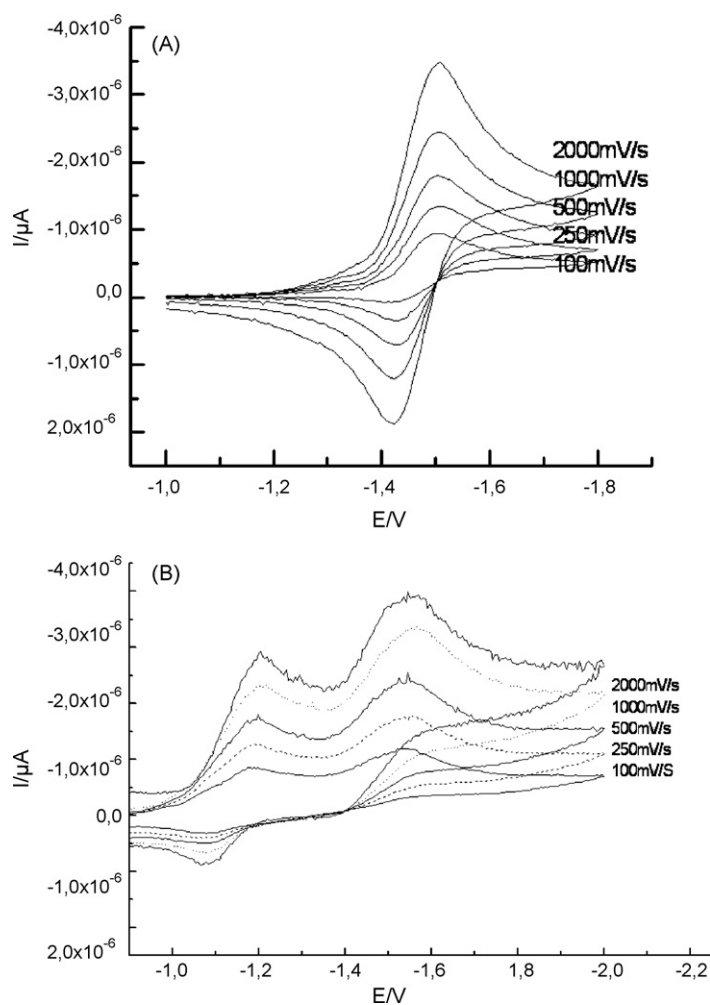


Fig. 2. (A) Cyclic voltammetry of compound **1** in DMSO obtained at the following sweep rates: 2000, 1000, 5000, 250 and 100 mV s^{-1} . (B) Cyclic voltammetry of compound **7** in DMSO obtained at the following sweep rates: 2000, 1000, 5000, 250 and 100 mV s^{-1} .

that could be assigned to one hydrogen atom of the triazolopyridine group. Molecules **2** and **4** (Fig. 4) were analyzed and simulated in term of one triplet of one nitrogen atom and two triplets due to two groups of two equivalent hydrogens. Molecules **3** was analyzed and simulated in term of one triplet of one nitrogen atom and one triplets due to two groups of two equivalent hydrogens and one doublet due to one equivalent hydrogen of the triazolepyridine ring. Molecule **5** showed a similar hyperfine pattern to the other triazolopyridyl pyridyl ketone group, ESR spectrum was analyzed in term of one triplet due to a one nitrogen atom with a large hyperfine constant and one triplet due to two equivalent hydrogens and two doublet due to one hydrogens belonging to the triazolopyridine ring and the other ones belonging to the pyridine ring. The same hyperfine pattern was found to the dicarbonyl derivative **10** (Fig. 5).

For compounds **6, 7** and **9** the ESR spectra were analyzed and simulated in terms of one triplet due to a one nitrogen atom which a large hyperfine constant and one triplet due to two equivalent hydrogens and one doublet due to one hydrogen. This hyperfine

Table 2
Experimental and theoretical hyperfine constants in gauss of studied compounds and g value

Molecule	aN	aN	aN	a2H	a2H	a2H	aH	aH	g Value
1 Exp DFT	1.2 (1)	0.22 (2)	0.15 (3)	0.7 (5,6)			4.5, 6.5 (7)		2.056
2 Exp DFT	4.8, 6.00 (1)	0.14 (2)	0.05 (3)	1.7, 1.95 (5,6)	2.5, 3.22 (4,7)				2.050
3 Exp DFT	4.8, 6.21 (1)	0.17 (2)	0.08 (3)	1.7, 2.22 (5,6)	2.5, 3.31 (4,7)				2.060
4 Exp DFT	4.8, 6.24 (1)	0.15 (2)	0.07 (3)	1.7, 2.20 (5,6)	2.5, 3.28 (4,7)				2.059
5 Exp DFT	8.0, 7.48 (1)	0.15 (2)	0.09 (3)	1.8, 2.61 (5,6)			1.5, 1.92 (7)	0.9, 0.75 (H pyridine ring)	2.061
6 Exp DFT	4.7, 6.00 (1)			1.7, 2.20 (2,3)			1.6, 1.90 (4)		2.057
7 Exp DFT	4.9, 6.1 (1)			1.7, 2.30 (2,3)			1.6, 1.88 (4)		2.061
8 Exp DFT	4.8, 6.20 (1)	4.2, 5.90 (2)	4.5, 6.00 (3)	2.6, 3.04 (5,6)	2.7, 2.95 (4,7)	2.5, 2.87 (8,9)		1.5, 1.96 (10)	2.055
9 Exp DFT	8.0, 7.34 (1)	0.18 (2)	0.08 (3)	1.7, 2.10 (5,6)			1.4, 1.09 (4)		2.056
10 Exp DFT	7.8, 7.0 (1)	0.19 (2)	0.08 (3)	1.7, 2.30 (5,6)			1.5, 2.05 (7)	0.9, 1.05 (H pyridine ring)	2.060

pattern indicated that the electron spin density was delocalized in the central pyridine ring of these molecules.

Finally, molecule **8** (Fig. 6) showed a different hyperfine pattern compared to those of molecules of this family. The ESR spectrum was analyzed in terms of three triplets due to three nitrogen atoms and three triplets due to three groups of two equivalent hydrogens and one doublet due to one hydrogen. This hyperfine pattern showed that the spin density delocalization will be in the triazolopyridine ring

3.3. Phase-solubility measurements

Two CDs enhanced the poor aqueous solubility of the compounds **4**, **6**, **7** and **11**, thus proving a certain degree

of its inclusion complexation in aqueous solutions. All phase-solubility diagrams of these molecules with β CD, and HP- β CD within the concentration range studied displayed a typical AL type diagram (i.e., linear increase of molecules solubility with increasing β CD, and HP- β CD concentration), consistent with a 1:1 molecular complex formation for two CDs. The result observed showed a linear behaviour which is unequivocal for all CDs studied ($r^2 = 0.996$ or better). The binding constant K_s of the complexes were calculated from the slopes of the linear phase-solubility plots according to the methodology described before. Results are summarized in Table 3. The K_s showed similar value in both CDs. However, small difference could be appreciated depending on the molecule included. The larger value found in molecules **11** and **4** compared to values in molecules **6** and **7** could indicate that the inclusion will be different. Meanwhile, in the complexes with molecules **6** and **7**

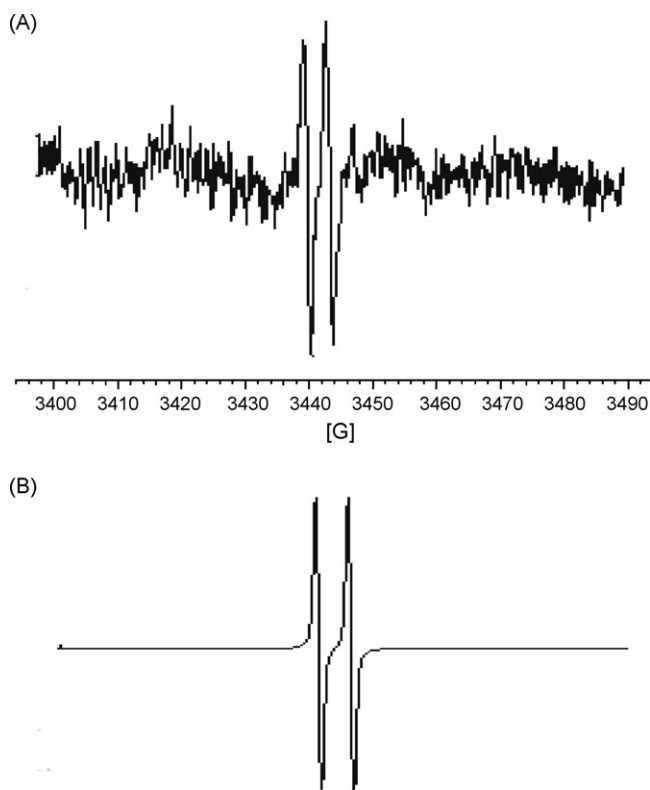


Fig. 3. (A) ESR experimental spectrum of the radical-anion of compound **1** in DMSO. Spectrometer conditions: microwave frequency, 9.68 GHz; microwave power, 20 mW; modulation amplitude, 0.2 G; scan rate, 1.25 G s⁻¹; time constant, 0.5 s; number of scans, 15. (B) Simulated spectrum.

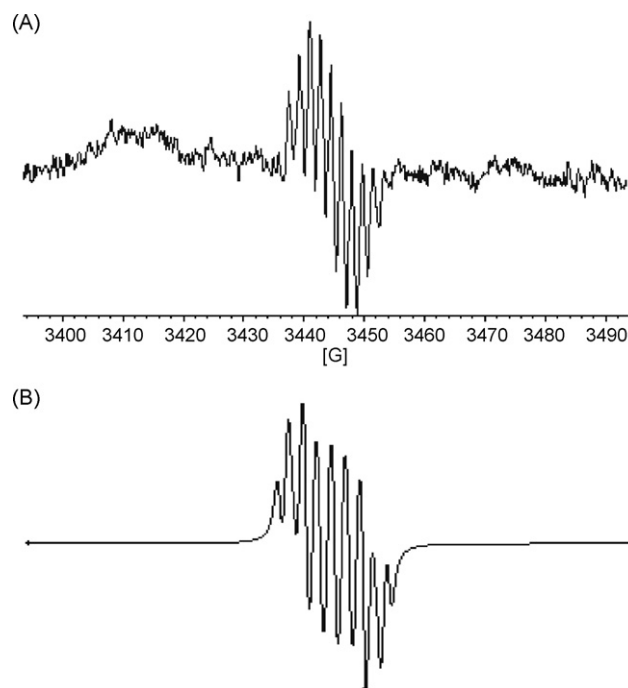


Fig. 4. (A) ESR experimental spectrum of the radical-anion of compound **4** in DMSO. Spectrometer conditions: microwave frequency, 9.68 GHz; microwave power, 20 mW; modulation amplitude, 0.2 G; scan rate, 1.25 G s⁻¹; time constant, 0.5 s; number of scans, 15. (B) Simulated spectrum.

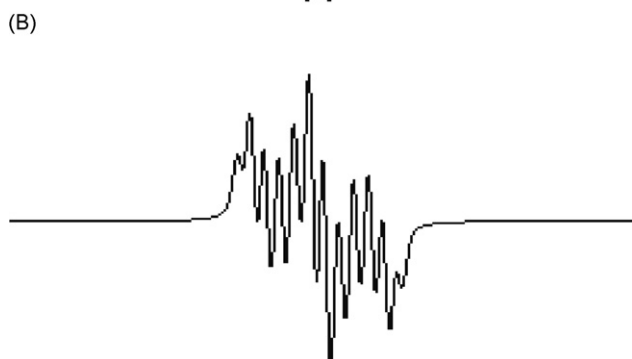
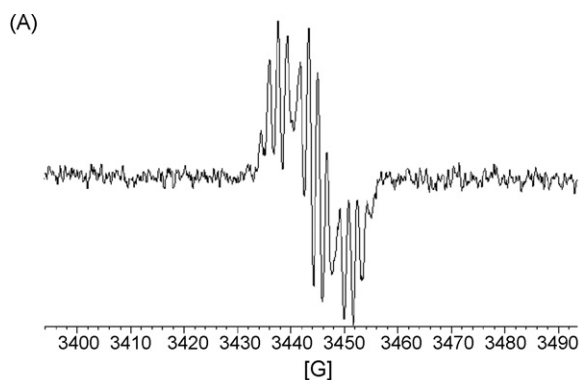


Fig. 5. (A) ESR experimental spectrum of the radical-anion of compound **10** in DMSO. Spectrometer conditions: microwave frequency, 9.68 GHz; microwave power, 20 mW; modulation amplitude, 0.2 G; scan rate, 1.25 G s⁻¹; time constant, 0.5 s; number of scans, 15. (B) Simulated spectrum.

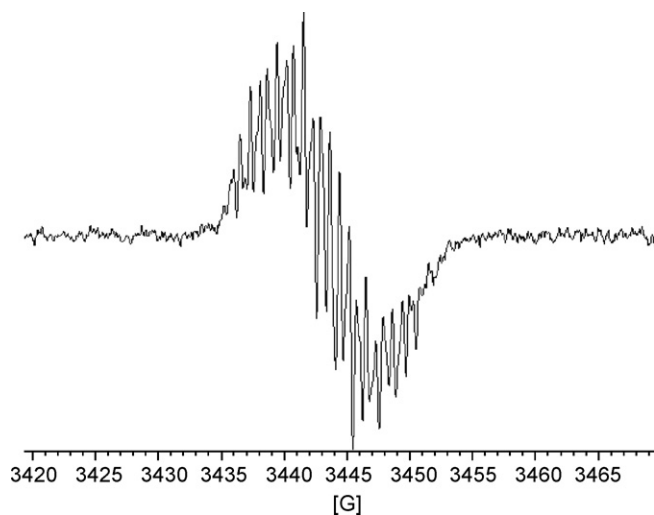


Fig. 6. ESR experimental spectrum of the radical-anion of compound **8** in DMSO. Spectrometer conditions: microwave frequency, 9.68 GHz; microwave power, 20 mW; modulation amplitude, 0.2 G; scan rate, 1.25 G s⁻¹; time constant, 0.5 s; number of scans, 15.

Table 3
Apparent stability constants (K_s) of **11**, **4**, **6**, and **7** molecules inclusion complexes

Molecules	β CD K_s (M ⁻¹)	HP- β CD K_s (M ⁻¹)
11	59	67
4	56	54
6	37	32
7	39	32

the triazolopyridine ring could be included in both CDs, however the complexes with molecules **11** and **4** remain included by pyridine ring.

3.4. Theoretical calculations

We fully optimized the geometries for the electron-paired and anion radical molecules at AM1 level. All radicals structures showed small distortion, respect to the neutral analogues molecules. B3LYP 6-31G* calculations were performed in order to obtain the theoretical hyperfine constants, using the geometries from AM1 calculations. Table 2 shows both the experimental and calculated hyperfine constants. These results are in agreement with the assignment of the hyperfine constants. Compounds **2**, **3** and **4** do not have the pyridine ring in the same plane of the triazolopyridine ring (around 46° between rings), however, molecule **1** showed 89° between these rings. The theoretical hyperfine coupling to compound **1** showed that the spin density are located in the triazolopyridine ring in particular in the hydrogen 8, in agreement with doublet obtained by ESR spectrum (Fig. 3), however for **2–5** and **10** molecules the theoretical hyperfine constant showed that spin density are more delocalized in one of the triazolopyridine ring. Respect to compounds **6**, **7** and **9** the spin density are localized in the central pyridine ring. Finally, molecule **8** showed that the spin density are localized mainly in the triazolopyridine ring however the electron unpair also is delocalized in pyridine rings in according the with the experimental ESR spectra.

4. Concluding remarks

The results obtained from the electrochemical studies showed a one step reduction mechanism for the one-carbonyl derivatives and two step for the dicarbonyl derivatives. The first wave for both families was assigned to the generation of the correspondent free radical species, and the second wave in the dicarbonyl family was assigned to the dianion derivatives. Stable free radicals were generated using electrochemical reductions at potential corresponding to first wave obtained from the voltametric experiments. The ESR spectra indicated that the spin density delocalization is depends on of the rings presented in the molecule.

The phase-solubility measurements indicated an interaction between molecules **4**, **6**, **7** and **11** and CDs in water. These inclusion complexes are 1:1 with β CD, and HP- β CD. The values of K_s showed a different kind of complexes depending on which rings are included. Finally, the theoretical results are in complete agreement with the experimental ones.

Acknowledgements

Our thanks are due to the Ministerio de Educación y Ciencia Project CTQ 2006-15672-C05-03/BQC and Vicerrectorado de Relaciones Internacionales de la Universidad de Valencia for a grant to C.O.-A.

References

- [1] L.-G. Feoktistov, in: M.M. Baizer, H. Lund (Eds.), *Organic Electrochemistry*, second ed., Marcel Dekker, New York, 1983, pp. 315–320.
- [2] (a) J.H. Stocker, R.M. Jenevein, D.H. Kern, *J. Org. Chem.* 43 (1969) 2807–2810;
(b) E.J. Rudd, B. Conway, *Trans. Faraday Soc.* 67 (1971) 440–447;
(c) L. Nadjo, J.M. Saveant, *J. Electroanal. Chem.* 44 (1973) 327–366;
(d) W.J.M. van Tilborg, D.J. Smit, J.R. Neth, *Chem. Soc.* 98 (1979) 532–536;
(e) J.E. Swartz, T.J. Mahachi, E. Kariv-Miller, *J. Am. Chem. Soc.* 110 (1988) 3622–3628;
(f) J.M. Tanko, R.E. Drumright, *J. Am. Chem. Soc.* 114 (1992) 1844–1854;
(g) L. Mattiello, L. Rampazzo, *J. Chem. Soc., Perkin Trans.* (1993) 2243–2247;
(h) E. Liotier, G. Mousset, *Can. J. Chem.* 73 (1995) 1488–1496.
- [3] G. Yang, S. Zheng, X. Chen, H.K. Lee, Y. Zhou, *Inorg. Chim. Acta* 303 (2000) 86–93.
- [4] A.C. Deveson, S.L. Heath, C.J. Harding, A.K. Powell, *J. Chem. Soc., Dalton Trans.* (1996) 3173–3178.
- [5] S.O. Sommerer, B.L. Westcott, J.A. Jircitano, A.K. Abboud, *Acta Crystallogr., Sect. C* 52 (1996) 1426–1428.
- [6] E.C. Constable, *Metal and Ligand Reactivity*, VHC, Weinheim, Germany, 1996, pp. 46, 47, 57–59.
- [7] A. Thoso, B. Dionyssopoulou, C. Raptopoulou, A. Terzis, E. Bakalbassis, S. Perlepes, *Angew. Chem. Int. Ed.* 38 (1999) 983–985.
- [8] G. Papaefstathiou, S. Perlepes, *Comments Inorg. Chem.* 23 (2002) 249–274.
- [9] A. Boudalis, B. Donnadieu, V. Nastopoulos, J. Clemente-Juan, A. Mari, Y. Sanakis, J.P. Tuchagues, S. Perlepes, *Angew. Chem. Int. Ed.* 43 (2004) 2266–2270.
- [10] (a) E.M. Kosower, E.J. Poziomek, *J. Am. Chem. Soc.* 86 (1964) 5515–5523;
(b) L. Grossi, F. Minisci, G.F. Pedulli, *J. Chem. Soc., Perkin Trans. 2* (1977) 943–947;
(c) L. Grossi, F. Minisci, G.F. Pedulli, *J. Chem. Soc., Perkin Trans. 2* (1977) 948–952.
- [11] P. Neta, L.K. Patterson, *J. Phys. Chem.* 78 (1974) 2211–2217.
- [12] N. Leventis, X. Gao, *J. Phys. Chem. B* 103 (1999) 5832–5836.
- [13] Y. Nakamura, N. Kamon, T. Hori, *Chem. Soc. Jpn.* 62 (1989) 551–557.
- [14] D.C. Bookbinder, M.S. Wrighton, *J. Electrochem. Soc.* 130 (1983) 1080–1085.
- [15] A.K. Boudalis, C.P. Raptopoulou, B. Abarca, R. Ballesteros, M. Chadlaoui, J.P. Tuchages, A. Terzis, *Angew. Chem. Int. Ed.* 45 (2006) 432–435.
- [16] C. Olea-Azar, B. Abarca, E. Norambuena, L. Opazo, C. Rigol, R. Ballesteros, M. Chadlaoui, *Spectrochim. Acta Part A* 61 (2005) 2261–2266.
- [17] M. Somi Reddy, M. Narender, K. Rao, *Tetrahedron Lett.* 46 (2005) 1299–1301.
- [18] M.D. Truppo, J. Kim, M. Broker, A. Madin, M.G. Sturr, J.C. Moore, *J. Mol. Catal. B: Enzym.* 38 (2006) 158–162.
- [19] B. Abarca, R. Ballesteros, M. Chadlaoui, *Tetrahedron* 60 (2004) 5785–5792.
- [20] B. Abarca, R. Ballesteros, M. Chadlaoui, *Arkivoc* vii (2008) 73–83.
- [21] B. Abarca, R. Ballesteros, M. Elmasnaouy, *Tetrahedron* 54 (1998) 15287–15292.
- [22] T. Higuchi, K.A. Connors, *Adv. Anal. Chem. Instr.* 4 (1965) 117–212.
- [23] R. Nicholson, I. Shain, *Anal. Chem.* 36 (1964) 706–723.